The Astrophysical Journal, 603:L61–L64, 2004 March 1

ON THE SELF-SIMILARITY OF UNSTABLE MAGNETIC DISCONTINUITIES IN SOLAR ACTIVE REGIONS

Loukas Vlahos[1] and Manolis K. Georgoulis[2]

Received 2003 December 23; accepted 2004 January 20; published 2004 February 12

ABSTRACT

We investigate the statistical properties of possible magnetic discontinuities in two solar active regions over the course of several hours. We use linear force-free extrapolations to calculate the three-dimensional magnetic structure in the active regions. Magnetic discontinuities are identified using various selection criteria. Independently of the selection criterion, we identify large numbers of magnetic discontinuities whose free magnetic energies and volumes obey well-formed power-law distribution functions. The power-law indices for the free energies are in the range $[-1.6, -1.35]$, in remarkable agreement with the power-law indices found in the occurrence frequencies of solar flare energies. This agreement and the strong self-similarity of the volumes that are likely to host flares suggest that the observed statistics of flares may be the natural outcome of a preexisting spatial self-organization accompanying the energy fragmentation in solar active regions. We propose a dynamical picture of flare triggering consistent with recent observations by reconciling our results with the concepts of percolation theory and self-organized criticality. These concepts rely on self-organization, which is expected from the fully turbulent state of the magnetic fields in the solar atmosphere.

Subject headings: Sun: activity — Sun: flares — Sun: magnetic fields

1. INTRODUCTION

Magnetic fields and the dissipation of magnetic energy are believed to be responsible for the observed solar activity. Small-scale energy release, such as may be found in the "confined" flare (Moore et al. 1980), may be triggered by the spontaneous formation of unstable magnetic discontinuities in solar active regions (ARs; Parker 1983, 1988). Magnetic discontinuities are formed and evolve either when the footpoints of the thin magnetic flux fibrils are shuffled by the continuous velocity field on the photosphere or when new magnetic flux emerges from the convection zone. The nonpotential (free) magnetic energy of these discontinuities is distributed within their volumes, which represent only a fraction of the total active region volume. Magnetic reconnection and subsequent dissipation are probably linked to a loss of equilibrium with respect to a *critical threshold*. This threshold might refer to, e.g., a critical current density j_c that, if locally exceeded, leads to current instabilities and heating due to the onset of anomalous resistivity (Papadopoulos 1977; Parker 1993). The details of the above physical process are still unknown. The formation of magnetic discontinuities and current sheets is a continuous process in ARs. While most of these discontinuities remain relatively stable (subcritical), a fraction of them may become unstable (critical), thus causing rapid magnetic reconnection that releases their free magnetic energy and provides the energy content for a flaring or subflaring event.

The concept of self-organized criticality (SOC; see Bak 1996) helped to refine the above picture (Lu & Hamilton 1991; Vlahos et al. 1995): An internal self-organization in solar ARs leads to the formation of a network of minimally stable magnetic structures. If one of these structures becomes unstable, it triggers a cluster of instabilities causing an avalanche-type energy release event. In the course of an avalanche, previously subcritical configurations may become critical, thus contributing to the flaring volume. The key elements in envisioning a dynamical picture of flare triggering were already in place before the introduction of SOC (i.e., critical thresholds, magnetic reconnection and field restructuring, anomalous resistivity and heating), but the missing link was the nonlinear formation of an avalanche. The outcome of SOC is extended scale invariance (power laws) in the frequency distributions of event sizes, in concert with the observations of Crosby, Aschwanden, & Dennis (1993) and numerous authors thereafter.

Occasionally, an avalanche may cause a global destabilization of the active region magnetic field structure, thus triggering an *ejective* flare (Svestka 1986) that might eventually drive a coronal mass ejection via, e.g., the *breakout* mechanism (Antiochos, DeVore, & Klimchuk 1999). The morphological diversity of the energy release process cannot be summarized by just a few flare categories. Nevertheless, a number of characteristic magnetic topologies have been traditionally viewed as sources of very large flares, such as the extended sheared arcades that trigger a *two-ribbon* flare (e.g., Priest & Forbes 2002). These relatively rare flares are not the subject of the present study, which focuses on the frequent, confined events.

A self-organization of the magnetic structures on the photosphere has been revealed in numerous statistical studies (Howard 1996 and references therein) and is reflected by their fractal character (Meunier 1999). Percolation theory, known to reproduce the formation of solar ARs (Seiden & Wentzel 1996; Vlahos et al. 2002; Fragos, Rantsiou, & Vlahos 2004), might account for these observations. Percolation is another self-organized (although noncritical) process and implies that the photospheric footpoint motion is probably not a random walk, as assumed repeatedly in the literature, but a more complex process dictated by the fractal character of the photospheric magnetic fields.

In this study, we focus on the possible self-organization of the volumes that are likely to host flares rather than on the flares themselves. To achieve this, we study the three-dimensional *non flaring* magnetic structure of solar ARs. We use various selection criteria to identify potentially unstable locations, and we apply linear force-free extrapolations to calculate the respective magnetic field configurations. We perform the analysis in two ARs observed using the Mees Solar Observatory's Imaging Vector Magnetograph (IVM; Mickey et al. 1996). The description of the method

[1] Department of Physics, University of Thessaloniki, 54 124 Thessaloniki, Greece.
[2] Johns Hopkins University Applied Physics Laboratory, 11100 Johns Hopkins Road, Laurel, MD 20723-6099.

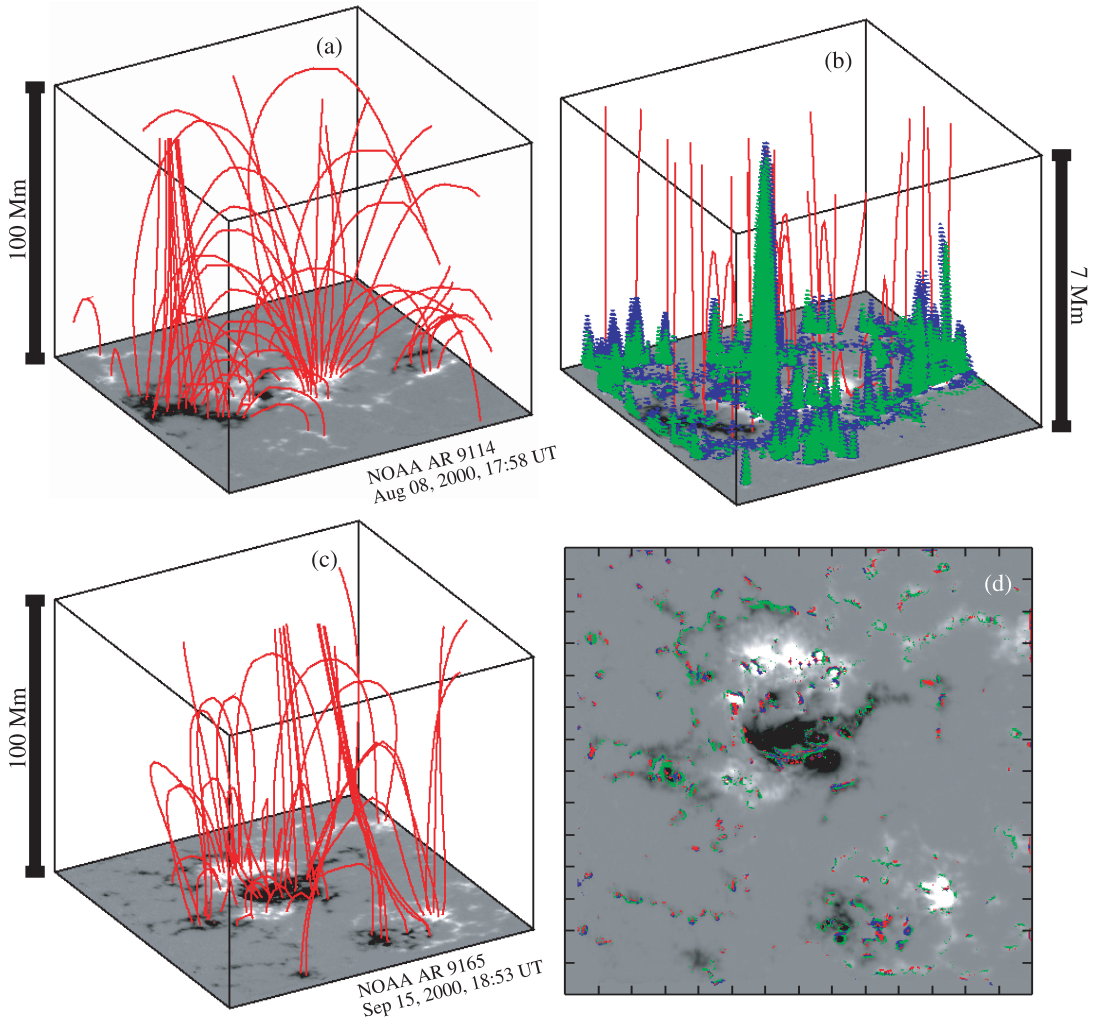

FIG. 1.—(*a*) Linear force-free field in NOAA AR 9114, calculated using $\alpha_{AR} = -1.39 \times 10^{-2}$ Mm^{-1}. (*b*) Lower part of the active region atmosphere. Shown are the magnetic field lines (*red*), with the identified magnetic discontinuities for Parker's angles of $\Delta\psi_c = 10°$ (*green*) and $\Delta\psi_c = 8°$ (*blue*). (*c*) Linear force-free field in NOAA AR 9165, calculated using $\alpha_{AR} = -1.89 \times 10^{-2}$ Mm^{-1}. (*d*) Projection of the detected magnetic discontinuities on the photosphere for $\Delta\psi_c = 14°$ (*red*) and $G_c = 0.2$ (*green*). Some selected locations satisfy both criteria (*blue*). The tick mark separation is 20″. The force-free parameters α_{AR} have been calculated using the minimum residual method (see § 2 for details).

is provided in § 2. In § 3 we apply the method to the IVM data, and in § 4 we discuss the implications of our findings.

2. ANALYSIS METHOD

Calculation of the coronal magnetic field.— Starting from an observed active region vector magnetogram, (1) we resolve the intrinsic azimuthal ambiguity of 180° (Georgoulis, LaBonte, & Metcalf 2004), and (2) we find the best-fit value α_{AR} of the force-free parameter for the entire AR, by minimizing the difference between the extrapolated and the ambiguity-resolved observed horizontal field (the "minimum residual" method of Leka & Skumanich 1999). We then perform a linear force-free extrapolation (Alissandrakis 1981) to determine the three-dimensional magnetic field in the AR. Although it is known that the magnetic fields on the photosphere are not force-free (Georgoulis & LaBonte 2004), we feel that a linear force-free approximation is suitable for our statistical purposes.

Selection criteria.—We apply two different selection criteria in order to identify potentially unstable locations. These refer to (1) Parker's angle and (2) the total magnetic field gradient. The angular difference $\Delta\psi$ between two adjacent magnetic field vectors, $\boldsymbol{B}_1$ and $\boldsymbol{B}_2$, is given by $\Delta\psi = \cos^{-1}[\boldsymbol{B}_1 \cdot \boldsymbol{B}_2/(B_1 B_2)]$. Assuming a cubic grid, we calculate six different angles at any given location, one for each of this location's closest neighbors. The location is considered potentially unstable if at least one $\Delta\psi_i > \Delta\psi_c$, where $i \equiv \{1, 6\}$ and $\Delta\psi_c = 14°$. The critical value $\Delta\psi_c$ refers to the Parker angle that, if exceeded locally, favors tangential discontinuities and the triggering of fast reconnection (Parker 1983, 1988). In addition, the total magnetic field gradient between two adjacent locations with magnetic field strengths B_1 and B_2 is given by $|B_1 - B_2|/B_1$. We calculate six different gradients at any given location. If at least one $G_i > G_c$, where $i \equiv \{1, 6\}$ and $G_c = 0.2$ (arbitrary choice), then the location is considered potentially unstable. A steep gradient of the magnetic field strength is thought to favor magnetic reconnection in three dimensions, in the absence of null points (Priest, Hornig, & Pontin 2003).

Estimation of the free magnetic energy.— Potentially unstable volumes are formed by adjacent selected locations. These volumes are given by $V = N\lambda^2\delta h$, where N is the number of adjacent locations, λ is the pixel size of the magnetogram, and

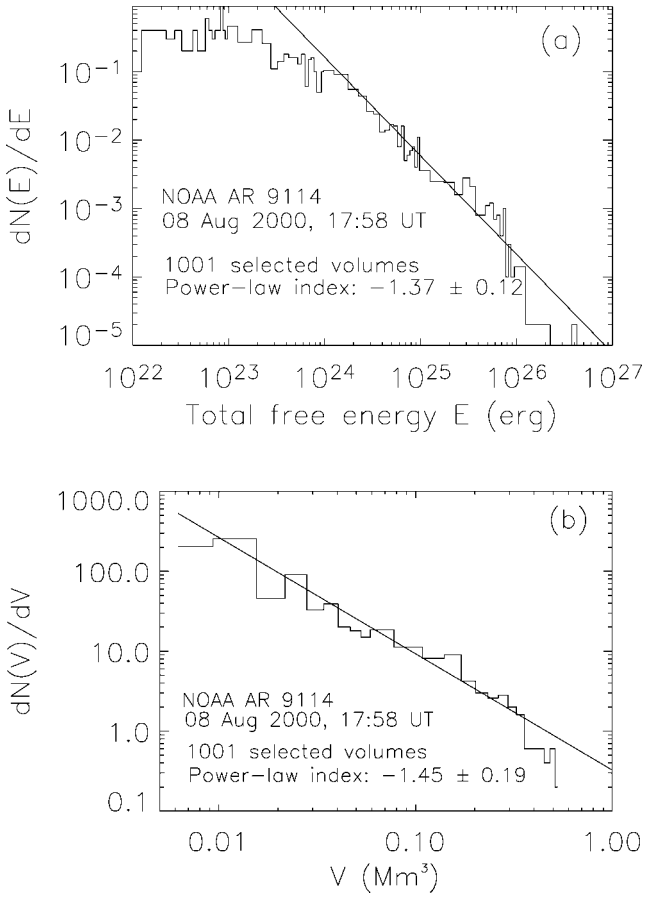

FIG. 2.—(*a*) Typical distribution function of the total free energy in volumes selected using a Parker angle $\Delta\psi_c = 14°$. (*b*) Respective distribution function of the selected volumes.

δh is the height step of the force-free extrapolation. The free magnetic energy E in any volume V is given by

$$E = \frac{\lambda^2 \delta h}{8\pi} \sum_{l=1}^{N} (\boldsymbol{B}_{\mathrm{ff},\,l} - \boldsymbol{B}_{p,\,l})^2, \qquad (1)$$

where $\boldsymbol{B}_{\mathrm{ff},\,l}$ and $\boldsymbol{B}_{p,\,l}$ are the linear force-free field and the potential field at location l, respectively. The assumption used is that any deviation from a potential configuration implies a nonzero free magnetic energy that is likely to be released if certain conditions are met.

3. RESULTS

The method is applied to two time series of active region vector magnetograms, namely, for NOAA ARs 9114 and 9165, observed by the IVM on 2000 August 8 and on 2000 September 15, respectively. The time series span over the IVM daily observing interval (from ~17:30 to ~22:30 UT). NOAA AR 9114 showed no flares/subflares during the observations, while AR 9165 was more dynamic, showing a number of subflares but no major flares. By choosing the above ARs, we study the statistics of the magnetic discontinuities independently of the activity in the AR. Extrapolations proceed up to a height of 100 Mm, with a step height $\delta h = 0.1$ Mm. The IVM pixel size is $\lambda = 0\farcs55 \simeq 0.396$ Mm, and hence a volume element is ~0.016 Mm^3.

Figures 1*a* and 1*c* show examples of the three-dimensional magnetic topology in NOAA ARs 9114 and 9165, respectively.

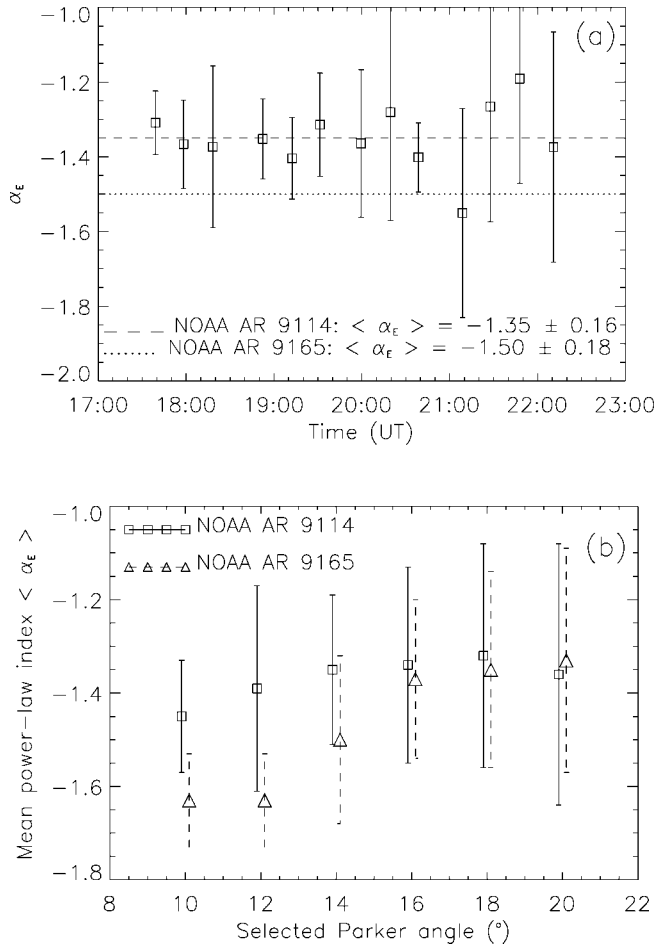

FIG. 3.—(*a*) Temporal variability of the power-law indices over the IVM observing interval. Statistics have been obtained using a Parker angle $\Delta\psi_c = 14°$. The points and error bars correspond to NOAA AR 1914. The mean power-law indices $\langle\alpha_E\rangle$ are indicated by a dashed line (NOAA AR 9114) and by a dotted line (NOAA AR 9165). (*b*) Mean power-law index $\langle\alpha_E\rangle$ for different definitions of the Parker angle. Rectangles and solid error bars correspond to NOAA AR 9114. Triangles and dashed error bars correspond to NOAA AR 9165.

In Figure 1*b*, we show a small portion of the atmosphere of Figure 1*a*, up to a height of 7 Mm. We identify 2394 potentially unstable volumes, shown for Parker's angles of $\Delta\psi_c = 10°$ (*green*) and $\Delta\psi_c = 8°$ (*blue*). For altitudes larger than 7 Mm, the smooth products of the extrapolation preclude the fulfillment of any of the selection criteria discussed in § 2. A similar situation exists at any given time for both ARs. In Figure 1*d*, we show the photospheric projection of 1387 potentially unstable volumes identified in NOAA AR 9165 for $\Delta\psi_c = 14°$ (*red*) and 2834 volumes identified for $G_c = 0.2$ (*green*). The blue areas indicate locations where both criteria are satisfied.

A typical distribution function of the total free energy in the selected volumes is given in Figure 2*a*. We obtain a well-defined power law extending over 2 orders of magnitude in the range [10^{24}, 10^{26}] ergs, with a power-law index $\alpha_E = -1.37 \pm 0.12$. Notice the close proximity of the power-law index with that of the total energy distribution of flares, known to vary between −1.4 and −1.6. If instabilities involve a random sample of these volumes, the total energy frequency distribution of the resulting flares should not be very different from the distribution of Figure 2*a*. The selected volumes also obey a power-law frequency distribution such as the one shown in Figure 2*b*. The power-law index is $\alpha_V = -1.45 \pm 0.19$. The noninteger value of the index

α_V illustrates the spatial fractality of the energy fragmentation process (McIntosh & Charbonneau 2001).

Figure 3*a* shows the variability of the power-law indices α_E over the entire observing interval when $\Delta\psi_c = 14°$. The points and error bars correspond to NOAA AR 9114, while the mean index values $\langle\alpha_E\rangle$ are indicated for both ARs. Although the error bars are not negligible, no systematic tendency with time appears in the values of α_E. The mean values $\langle\alpha_E\rangle$ for NOAA ARs 9114 and 9165 are -1.35 ± 0.16 and -1.50 ± 0.18, respectively. For $G_c = 0.2$, we obtain $\langle\alpha_E\rangle = -1.50 \pm 0.23$ and $\langle\alpha_E\rangle = -1.61 \pm 0.1$, respectively. All indices are in excellent agreement with numerous flare observations. Of particular interest is whether power-law indices change when the critical thresholds of the selection criteria change. In Figure 3*b*, we have performed this test for both ARs for different values of $\Delta\psi_c$. Very similar results are obtained when the threshold G_c changes. Although within error bars, we find a weak dependence between $\langle\alpha_E\rangle$ and $\Delta\psi_c$. For lower $\Delta\psi_c$, when the number of selected volumes increases and the total free energy distribution extends mostly toward lower energies, the power-law indices become steeper. This might favor a nanoflaring scenario with numerous small events obeying steeper power laws, but clearly more investigation is required on this point. For moderate choices of $\Delta\psi_c$ centered around 14°, $\langle\alpha_E\rangle$ is fully consistent with flare observations.

4. DISCUSSION AND SUMMARY

We present evidence of a strong self-similarity of the possible magnetic discontinuities in solar ARs. Potentially unstable volumes may well be self-organized, as suggested by percolation and SOC concepts. This study suggests that the intrinsic self-similarity found in the distribution functions of flare parameters is a direct outcome of the self-similarity of the volumes hosting the flares. The proximity between the power-law indices in the distribution functions of the free energies and those of the frequency distributions of flare energies implies an approximate one-to-one conversion of the free magnetic energy into thermal energy in flare-type processes. In particular, we find that (1) a complex network of potentially unstable volumes exists for both studied ARs, independently of their activity and for the entire observing interval, (2) these volumes are preferentially located close to the photosphere, so the energy release may be enhanced at low altitudes ($\lesssim$10 Mm; Aschwanden, Schrijver, & Alexander 2001), (3) the distribution functions of these volumes as well as of their total free energies are power laws with indices $\alpha_V \simeq -1.5$ and $\alpha_E \in [-1.6, -1.35]$, respectively, (4) the above power-law indices depend weakly on the selection criterion and the critical threshold, with a tendency to become flatter as the selection criterion becomes more stringent, and (5) the maximum free energies of the selected volumes are of the order $\sim 10^{27}$ ergs. This implies a nonlinear interaction of a large number of volumes to provide a large flare with energy, say, $\sim 10^{30}$ ergs, suggestive of a SOC-type avalanche occurring probably on *magnetic separatrices* (Démoulin & Priest 1997) and giving rise to a "tectonic" behavior such as the one discussed by Schrijver & Title (2002).

Self-organization appears essential for the formation and evolution of solar ARs. While noncritical self-organization (e.g., percolation) may regulate the emergence and evolution of solar ARs, critical self-organization (e.g., SOC) may determine the energy release process. The nature of the critical threshold(s) (electric current density, angular difference, field strength gradient) remains elusive. Energy release in the form of flares cannot be accomplished unless nonlinear interaction or intercommunication between individual energy release sites is at work. In essence, solar ARs are an externally driven, self-organized nonlinear dynamical system, subject to a self-similar external driver such as the one modeled by Georgoulis & Vlahos (1996). Energy release can occur anywhere in the atmosphere, and it might be enhanced at low altitudes according to the situation (see, e.g., the discussion of Priest, Heyvaerts, & Title 2002). Self-organization and the cascading nature of solar flares are the natural outcome of the fully developed turbulent state in the active region atmosphere (Biskamp 1993; Einaudi et al. 1996).

As a simple paradigm, imagine the free magnetic energy in an AR as explosives stored in a warehouse. The spatial distribution of the explosives in the warehouse is crucial when a fire breaks out in one particular spot. If this spot is isolated, the explosion will be small-scale, and the damage will be insignificant. If stacks of explosives exist near the spot of the initial explosion, then a domino effect will occur, and the entire stock will be destroyed.

We are grateful to B. J. LaBonte, for contributing the IVM magnetograms. Data used here from the Mees Solar Observatory, University of Hawaii, are produced with the support of NASA and AFRL grants. This work has received partial support from NSF grant ATM-0208104 and from the Research Training Network (RTN) "Theory, Observation and Simulation of Turbulence in Space Plasmas," funded by the European Commission (contract HPRN-eT-2001-00310).

REFERENCES

Alissandrakis, C. E. 1981, A&A, 100, 197
Antiochos, S. K., DeVore, C. R., & Klimchuk, J. A. 1999, ApJ, 510, 485
Aschwanden, M. J., Schrijver, C. J., & Alexander, D. 2001, ApJ, 550, 1036
Bak, P. 1996, How Nature Works (New York: Springer)
Biskamp, D. 1993, Nonlinear Magnetohydrodynamics (Cambridge: Cambridge Univ. Press)
Crosby, N. B., Aschwanden, M. J., & Dennis, B. R. 1993, Sol. Phys., 143, 275
Démoulin, P., & Priest, E. R. 1997, Sol. Phys., 175, 123
Einaudi, G., Velli, M., Politano, H., & Pouquet, A. 1996, ApJ, 457, L113
Fragos, T., Rantsiou, M., & Vlahos, L. 2004, A&A, in press
Georgoulis, M. K., & LaBonte, B. J. 2004, ApJ, submitted
Georgoulis, M. K., LaBonte, B. J., & Metcalf, Th. R. 2004, ApJ, 602, 447
Georgoulis, M. K., & Vlahos, L. 1996, ApJ, 469, L135
Howard, R. F. 1996, ARA&A, 34, 75
Leka, K. D., & Skumanich, A. 1999, Sol. Phys., 188, 3
Lu, E. T., & Hamilton, R. J. 1991, ApJ, 380, L89
McIntosh, S. W., & Charbonneau, P. 2001, ApJ, 563, L165
Meunier, N. 1999, ApJ, 515, 801
Mickey, D. L., Canfield, R. C., LaBonte, B. J., Leka, K. D., Waterson, M. F., & Weber, H. M. 1996, Sol. Phys., 168, 229
Moore, R., et al. 1980, in Solar Flares: A Monograph from *Skylab* Solar Workshop II, ed. P. Sturrock (Boulder: Colorado Assoc. Univ. Press), 341
Papadopoulos, K. 1977, Rev. Geophys. Space Phys., 15, 113
Parker, E. N. 1983, ApJ, 264, 642
———. 1988, ApJ, 330, 474
———. 1993, ApJ, 414, 389
Priest E. R., & Forbes, T. G. 2002, A&A Rev., 10, 313
Priest, E. R., Heyvaerts, J. F., & Title, A. M. 2002, ApJ, 576, 533
Priest, E. R., Hornig, G., & Pontin, D. I. 2003, J. Geophys. Res. Space Phys., 108(A7), 1285
Schrijver, C. J., & Title, A. M. 2002, Sol. Phys., 207, 223
Seiden, P. E., & Wentzel, D. G. 1996, ApJ, 460, 522
Svestka, Z. 1986, in The Lower Atmosphere of Solar Flares, ed. D. F. Neidig (Tuscon: Univ. Arizona Press), 332
Vlahos, L., Fragos, T., Isliker, H., & Georgoulis, M. 2002, ApJ, 575, L87
Vlahos, L., Georgoulis, M., Kluiving, R., & Paschos, P. 1995, A&A, 299, 897